

The Evolutionary Ecology of Individual Foraging Decisions

Pratik R. Gupte^{1,*}

Christoph F. G. Netz¹

Franz J. Weissing¹

1. University of Groningen, Groningen 9747AG, The Netherlands.

* Corresponding authors; e-mail: p.r.gupte@rug.nl

Manuscript elements: EXAMPLE: Figure 1, figure 2, table 1, online appendices A and B (including figure A1 and figure A2). Figure 2 is to print in color.

Keywords: Examples, model, template, guidelines.

Manuscript type: Article.

Prepared using the suggested L^AT_EX template for *Am. Nat.*

Abstract

Understanding the causes and consequences of animal movement is key to mechanistically linking individual behaviour with population-level patterns. Classical models of individual-to-population foraging distributions do not account for the complex and changeable resource landscapes animals must navigate. Neither are the rich behavioural repertoires addressed that animals may exhibit in a foraging context, and their evolution is almost entirely ignored. We take a spatially explicit, individual-based simulation approach to model the evolution of individual movement and foraging strategies, and its consequences for population distributions in three simple foraging scenarios of increasing behavioural complexity. We show that movement rules and individual foraging strategies co-evolve to optimality in all three scenarios. We find that exploitation competition is a relatively weak driver of individual movement and intake, and that this effect depends on the replenishment rate of the resource. We also find that when interference competition in the form of kleptoparasitism is allowed, it gives rise to a quasi-predator class of individuals and a third trophic level emerges. These quasi-predators compete among themselves much more than they compete with all other individuals, even when they are able to switch from a scrounger to a producer strategy.

WIP.

Introduction

Evolutionary Simulation Model of Individual Foraging Decisions

Our model is an individual-based evolutionary simulation whose most basic components — the environment size and shape, its gridded structure and each cell’s capacity to hold multiple individuals, as well as the discrete conception of time within and between generations — is taken from Netz et al. *in prep.*. We conceptualised the model and the scenarios around the behaviour of waders (*Charadrii*, and especially oystercatchers *Haematopus sp.*), which are extensively studied in an optimal foraging context (e.g. Ens et al., 1990; Vahl et al., 2005*a,b,c*). We simulated a fixed population with a fixed size of 10,000 individuals moving on a landscape of 512^2 grid cells, with the landscape wrapped at the boundaries so that individuals passing beyond the bounds at one end re-appear on the diametrically opposite side. Individuals have a lifetime of T timesteps, with T set to 400 by default. After their lifetime, individuals reproduce and transmit their heritable traits proportional to their fitness over their lifetime. The model code (in C++) can be found as part of the Supplementary Material in the Zenodo repository at **Zenodo/other repository here**.

Flexibility in Foraging Strategies

Our model considers three main scenarios of flexibility in individual foraging strategies. The **first scenario** is an inflexible producer-only case, in which individuals move about on the landscape and probabilistically find and consume discrete prey food items. Between finding and consuming a food item, individuals must ‘handle’ the prey for a fixed handling time T_H which is constant across prey items. Prey handling time T_H is set at 5 timesteps by default. The handling time dynamic is well known from many systems; for instance, it could be the time required for a wader to break through a mussel shell, with the handling action obvious to nearby individuals, and the prey not fully under the control of the finder. We refer to such individuals as ‘handlers’ for convenience. Handlers are assumed to be fully absorbed in their processing of prey, and do

not make any movements until they have fully handled and consumed their prey. The **second scenario** is a fixed-strategy case which adds some flexibility. Individuals at the start of their lifetime each choose between two foraging strategies, which are then fixed through life. The strategy choice is based on local environmental cues, and is covered in “Movement and Foraging Decisions”. The two strategies are to produce, i.e., to probabilistically find, handle, and consume discrete prey (as in the producer-only case), or to scrounge as a kleptoparasite, i.e., to steal a found prey item from the individual handling it. We refer to such scroungers as ‘kleptoparasites’ from here onwards. Kleptoparasites can steal from any handler, regardless of whether that handler acquired its prey by searching or theft. Kleptoparasites are always successful in stealing from the handler they target; this may be thought of as the benefit of the element of surprise, a common observation in nature. Having acquired prey, a kleptoparasite need only handle it for $T_H - t_h$ timesteps, where t_h is the time that the prey has already been handled by its previous handler. The targeted handler deprived of its prey is assumed to flee from the area, and does not make a further movement decision. Thus kleptoparasites clearly save time on handling compared to a producer, and the time saved increases with the handling time T_H of the prey. The **third scenario** is a flexible-strategy case, and individuals are allowed to be plastic in their foraging strategies, and choose between producing and scrounging strategies in each timestep. Apart from the frequency of the choice, the actual foraging dynamics are the same as described in the fixed-strategy case. Individuals move about on the environment, and each foraging strategy choice is based on local environmental cues (see “Movement and Foraging Decisions”).

Movement and Foraging Decisions

Individuals essentially use cues available in timestep t to predict their best move for the next timestep $t + 1$, and the strategy associated with that move (when this is allowed). The movement decision is based on three local environmental cues: (1) the number of discrete prey items G , (2) the number of individuals handling prey H (referred to as ‘handlers’), and (3) the number of individuals not handling prey P (referred to as ‘non-handlers’). The notation is chosen in keeping

with Netz et al. *in prep.*. These cues are available to individuals in all three model scenarios. Individuals occupy a single grid cell on the environment at a time, and assign a suitability score S incorporating G , H , and P per cell to the nine cells in their Moore neighbourhood (including their current cell). Following Netz et al. *in prep.*, individuals calculate the cell-specific S as

$$S = m_g G + m_h H + m_p P + m_b$$

where the weighing factors for each cue m_g , m_h and m_p , and the bias m_b are genetically encoded and heritable between generations. Individuals rank their Moore neighbourhood by S in timestep t and move to the highest ranked cell in timestep $t + 1$.

Individuals in the producers-only case make no foraging decisions and find food items probabilistically (see “Prey Environment and Ecological Dynamics”). In the fixed-strategy case, individuals pick a lifelong foraging strategy in their first timestep (t_0), while in the flexible-strategy case, individuals pick a strategy in each timestep t to be deployed in $t + 1$. Individuals in these latter two cases process the cell-specific environmental cues G , H , and P to determine their foraging strategy F for life (fixed strategy), or in the grid cell into which they have chosen to move in $t + 1$ (flexible strategy). F is determined as

$$F = \begin{cases} \text{producer,} & \text{if } f_g G + f_h H + f_p P + f_b \geq 0 \\ \text{scrounger,} & \text{otherwise} \end{cases}$$

where the cue weights f_g , f_h and f_p , and the bias f_b are also genetically encoded and heritable between generations.

In both latter cases that allow for kleptoparasitism, individuals make their foraging strategy choice for the next timestep after they have passed through the ecological dynamics of their current location. This excludes individuals that have been stolen from are an important exception; these fleeing agents are moved to a random cell within a Chebyshev distance of 5, and do not make a foraging decision there. Thus kleptoparasitism not only gains individuals prey items while depriving the targeted individual, it also displaces a potential competitor. All individu-

als move simultaneously, and attempt to implement the foraging strategy chosen for their new location (see below).

Prey Environment and Ecological Dynamics

Since our model was initially conceived to represent foraging waders, we developed a resource landscape based on mussels (family *Mytilidae*) that are commonly found in inter-tidal systems. Mussels beds share some important characteristics with other discrete prey items. Firstly, mussels are immobile relative to their consumers, and their abundances are largely driven by extrinsic environmental gradients and very small-scale interactions (de Jager et al., 2020, 2011). Secondly, in common with many ecological systems (Levin, 1992), mussels are not uniformly distributed across the inter-tidal mudflats, and are instead strongly spatially patterned into clusters ('beds') (de Jager et al., 2020, 2011). Thirdly, while prey or their signs in an area are often visible to consumers, consumers are not always certain of obtaining one of these prey, since prey can show small-scale anti-predator avoidance responses.

We captured these essential aspects of prey dynamics when implementing the resource landscape on which our individuals move. We modelled relative prey immobility and extrinsically driven abundance by assigning each grid cell of the resource landscape a constant probability of generating a new prey item per timestep, which we refer to as the growth rate r . We modelled clustering in the abundance of prey by having the distribution of r across the grid cells take the form of 1,024 uniformly distributed resource peaks with r declining from the centre of each peak to its periphery (Figure X). Effectively, the cell at the centre of each patch generates a prey item five times more frequently than the cells at the edges. Thus for a simulation-specific baseline $r_{base} = 0.03$, the central cell of a resource peak would have an $r_{centre} = 0.03$, and generate 3 items every 100 timesteps, compared with $r_{edge} = 0.006$, or 0.6 items generated in 100 timesteps. We ran the simulation with r_{base} values of 0.001, 0.01, 0.03, and 0.05, which we considered a sufficiently broad range. Cells in our landscape were modelled as being able to hold a maximum of K prey items, with the default $K = 5$. While a cell is at carrying capacity its r is 0. We modelled near-

perfect intermediate-range perception but uncertain short-range acquisition of prey by allowing individuals to perceive all prey items G in a cell, but giving individuals which choose a producer strategy only a probability of finding one of these prey. The probability of finding a prey item $p(success)$ is given as the probability of not finding any of G prey

$$p(success) = 1 - (1 - p_i)^G$$

where p_i is the detection probability of each of G items, which is uniformly set to 0.2 by default for all items.

Since we model foraging events as occurring simultaneously, it is possible for more producers to be considered successful in finding prey than there are discrete items in that cell. We resolve this simple case of exploitation competition by assigning G prey among some N successful finders at random. Producers that are assigned a prey item in timestep t begin handling it, and are considered to be handlers for the purposes of timestep $t + 1$ (primarily movement and foraging decisions of other individuals). It is important to note that a producer that has converted into a handler in timestep t is not an available target for kleptoparasites until timestep $t + 1$. Producers that are not assigned a prey item are considered idle during timestep t , and are counted as non-handlers for $t + 1$.

Kleptoparasites in the fixed- or flexible-strategy case face a slightly different challenge. All kleptoparasites in a cell successfully steal from a handler, contingent on the number of handlers matching or exceeding the number of kleptoparasites in timestep t . When the number of kleptoparasites exceeds handlers, handlers are assigned among kleptoparasites at random. Successful kleptoparasites convert into handlers, and similar to producer-handlers are unavailable as targets to other kleptoparasites until the next timestep. Unsuccessful kleptoparasites are considered idle, and are also counted as non-handlers for timestep $t + 1$. A handler that finishes processing its prey in timestep t returns to the non-handler state and is assessed as such by other agents when determining movements for $t + 1$.

Individuals move and forage on the resource landscape for T timesteps per generation, and

144 T is set at 400 by default. Handling a food item requires a maximum of T_H timesteps, during
145 which the handler is immobile.

146 *Reproduction and the Evolution of Decision Making*

147 At the end of each generation, the population is replaced by its offspring, maintaining the fixed
148 population size, and the decision-making weights which determine individual movement (m_g ,
149 m_h , m_p , m_b) and foraging strategy choice (f_g , f_h , f_p , f_b) are transmitted from parent individuals
150 to offspring. The number of offspring of each parent is proportional to the parent's share of the
151 population fitness, and this is implemented as a weighted lottery that selects a parent for each
152 offspring. The total lifetime intake of individuals is used as a proxy of fitness, and the popu-
153 lation's total fitness is its total intake. The decision-making weights are subject to independent
154 random mutations with a probability of 0.001. The size of the mutation (either positive or nega-
155 tive) is drawn from a Cauchy distribution with a scale of 0.01 centred on the current value of the
156 weight to be mutated. This allows for a small number of very large mutations while the majority
157 of mutations are small. Autocorrelation in the landscape coupled with limited natal dispersal
158 can lead to spatial heterogeneity becoming fixed in populations, as lineages adapt to local con-
159 ditions. Among other things, this could lead to population-level movements due to differential
160 reproduction that mirror shifts in resource abundance, rather than individual movement. To en-
161 sure individual movement rules evolved, we initialised each offspring at a random location on
162 the landscape, and also reset its total intake to zero.

163 *Simulation Output and Analysis*

164 *Spatial Distribution of Individuals, their Intake, and Prey Items.* Over each of the last eight gen-
165 erations of the simulation (991 – 998), we summed the following for each grid cell ij over the
166 generation's timesteps: (1) the number of prey items G , (2) the number of individuals following
167 each of the two strategies, producer N_p or kleptoparasitic scrounger N_s , and (3) the intake (in

food items consumed after handling) by agents following each of the two strategies, producer I_p or kleptoparasite I_s . For instance, the number of producer individuals in a generation to inhabit a cell ij would be

$$N_p = \sum_{t=0}^{i=T} n_{p_t}$$

where $t \in (0, 1 \dots T = 400)$, and n_{p_t} is the number of producers in cell ij at each timestep t . We saved this generation- and simulation- specific data to file, and these data are available at the Zenodo/IRODS repository at **Zenodo/other link here**. The volume of data at this stage was comparable to a very high-resolution, long-term ecological study, and we handled it accordingly. First, we processed the data to get the timestep-averaged values of G , N_p , N_s , I_p , and I_s for each cell, dividing each value by T (400). From this data, we calculated the per-capita intake rate (I per t) on each cell for each of the two strategies separately, which we denote as R_p (producers) and R_s (scroungers). We plotted the timestep- and generation-averaged item count (G), strategy count (N_p , N_s), and absolute and per-capita intake (I_p , I_s , and R_p , R_s) in relation to grid-cell quality (the growth rate, r) to investigate the spatial distribution of individuals (see Figure X).

Generalised Functional Response. In our simulation, individuals perceive and respond to the standing stock of prey items G on a cell rather than its growth rate r . This standing stock is unpredictable due to consumption by other individuals. To understand the consequences of movement, we need to investigate how individual intake rate varies with G as well as the presence of potential competitors. Thus we examined the generalised functional response (W) *sensu* Meer and Ens (1997). We plotted the per-capita intake rate achieved by individuals on grid-cells with similar numbers of prey items (G) and individuals ($N_p + N_s$) (see Figure Xa). We did this separately for W_p and W_s , the generalised functional response of individuals using the producer and kleptoparasitic scrounger respectively (see Figure Xb, Xc). We modelled the effect of competition and resource availability on W_p and W_s using a simple generalised linear model (GLM) with either W_p or W_s as the response, and the number of individuals and the number of prey items as the only additive predictors. We repeated this for simulations with different

baseline growth rates r , and examined variation in the contribution of competition and resource availability in the **form of the linear model coefficients of individual density and item density, respectively (see Figure X)**. These linear models took the form

$$W = \beta_0 + \beta_1 G + \beta_2 (N_p + N_s)$$

where W is either W_p or W_s . We fit these models for each r_{base} separately, but did not distinguish between replicates.

Decision Making Weights. To understand the evolutionary consequences of our simulation, we exported the the decision-making weights which determine individual movement (m_g, m_h, m_p, m_b) and foraging strategy choice (f_g, f_h, f_p, f_b) of each individual in every generation of the simulation. We examined how the frequency of these weights changed over the simulation, i.e., how the weights evolved. We visualised weights' evolution after scaling them between -1 and +1 using a hyperbolic tangent function, and binning the scaled values into intervals of 0.1. We refer to these scaled and binned values as phenotypes for convenience. Weights at or near -1 would represent the maximum evolved avoidance of an environmental cue (in relation to a movement weight) or the greatest evolved negative effect of a cue on choosing the foraging strategy (in relation to a strategy choice weight). Similarly, weights at or near +1 represent the greatest evolved preference for or positive effect of a cue on the movement and strategy choice mechanism of an individual.

Simulation Model Outcomes

Emergence of a Dynamic Equilibrium

WIP.

Evolution of Decision Making Weights

216 *Scenario 1: The Producers-Only Case.*

217 *Scenario 2: The Fixed Strategy Case.*

218 *Scenario 3: The Flexible Strategy Case.*

219 *Spatial Distribution of Individuals and Prey*

220 *Individual Distributions.* There number of individuals on a cell increased with its growth rate r ,
221 but there was substantial variation across cells with the same r . This variation was larger with
222 increasing r since there were fewer cells with higher r . In the producer-only case, individual
223 abundance showed a linear increase with cell quality, with the slope increasing with the simula-
224 tion growth rate r_{base} . When two strategies were allowed however, there were strong differences
225 in how they were distributed across cell qualities. In the fixed-strategy case, the abundance of
226 producer individuals was uniformly low across cell qualities, while the abundance of scrounging
227 kleptoparasites had a sigmoidal relationship with quality, mediated by r_{base} . In the flexible-
228 strategy case, the use of either strategy was nearly invariant with cell quality. At very low r_{base}
229 (0.001) the kleptoparasitic strategy was more often used than the producer strategy, while at
230 higher r_{base} , the producer strategy was more common across cell quality.

231 *Consequences for Prey Item Distribution.* The distributon of items G varied considerably between
232 scenarios and simulation-specific baseline growth rates r_{base} . In the **first scenario** G was insensi-
233 tive to r , and items were uniformly distributed across cells of different growth rates. G was not
234 significantly different among simulations with different r_{base} . In the **second scenario** G increased
235 strongly with r , and the curve of $G r$ varied with r_{base} . The $G r$ transformed from roughly linear
236 ($r_{base} = 0.001$), to exponential ($r_{base} = 0.01$), and finally to sigmoidal ($r_{base} \in 0.03, 0.05$) [see Figure
237 X]. In the **third scenario** G varied only weakly across cells with different r , and the $G r$ response
238 had a positive slope only for the highest r_{base} of 0.03 and 0.05.

Generalised Functional Response

The model coefficients of G and $N_p + N_s$ changed non-linearly in relation to r_{base} (Figure X). In the producers-only case, the coefficient β_2 increased with r_{base} when $r_{base} \leq 0.03$, after which it decreased below zero for $r_{base} = 0.25$. Similarly, the coefficient of items β_1 was highest at $r_{base} = 0.03$, decreasing to zero for $r_{base} = 0.1$ and 0.25 . In the fixed-strategy case, β_1 (items) was at or near zero across all r_{base} . However, β_2 for both W_p and W_s was near zero for $r_{base} \leq 0.05$, positive for $r_{base} \in 0.075, 0.1$, and zero for $r_{base} = 0.25$. Both in the flexible-strategy case, both β_1 and β_2 showed a hump-shaped relationship with r_{base} for both W_p and W_s , with the highest values at intermediate growth rates.

Discussion

Conclusion

Acknowledgments

The authors thank Hanno Hildenbrandt for contributing to the coding of the simulation model *Kleptomove*; Matteo Pederboni for contributing to the initial stages of the simulation model; and members of the Modelling Adaptive Response Mechanisms Group and of the Theoretical Biology department at the University of Groningen for helpful discussions on the manuscript.

Literature Cited

de Jager, M., J. van de Koppel, E. J. Weerman, and F. J. Weissing. 2020. Patterning in Mussel Beds Explained by the Interplay of Multi-Level Selection and Spatial Self-Organization. *Frontiers in Ecology and Evolution* 8.

- 259 de Jager, M., F. J. Weissing, P. M. J. Herman, B. A. Nolet, and J. van de Koppel. 2011. Lévy
260 Walks Evolve Through Interaction Between Movement and Environmental Complexity. *Science*
261 332:1551–1553.
- 262 Ens, B. J., P. Esselink, and L. Zwarts. 1990. Kleptoparasitism as a problem of prey choice: A study
263 on mudflat-feeding curlews, *Numenius arquata*. *Animal Behaviour* 39:219–230.
- 264 Levin, S. A. 1992. The Problem of Pattern and Scale in Ecology: The Robert H. MacArthur Award
265 Lecture. *Ecology* 73:1943–1967.
- 266 Meer, J. V. D., and B. J. Ens. 1997. Models of Interference and Their Consequences for the Spatial
267 Distribution of Ideal and Free Predators. *The Journal of Animal Ecology* 66:846.
- 268 Vahl, W. K., T. Lok, J. van der Meer, T. Piersma, and F. J. Weissing. 2005a. Spatial clumping of
269 food and social dominance affect interference competition among ruddy turnstones. *Behavioral*
270 *Ecology* 16:834–844.
- 271 Vahl, W. K., J. van der Meer, F. J. Weissing, D. van Dulleman, and T. Piersma. 2005b. The
272 mechanisms of interference competition: Two experiments on foraging waders. *Behavioral*
273 *Ecology* 16:845–855.
- 274 ———. 2005c. The mechanisms of interference competition: Two experiments on foraging
275 waders. *Behavioral Ecology* 16:845–855.

276

Appendix A: Supplementary Figures

277

Fox–dog encounters through the ages

Appendix B: Additional Methods

Measuring the height of fox jumps without a meterstick

Tables

281

Figure legends

282

Online figure legends

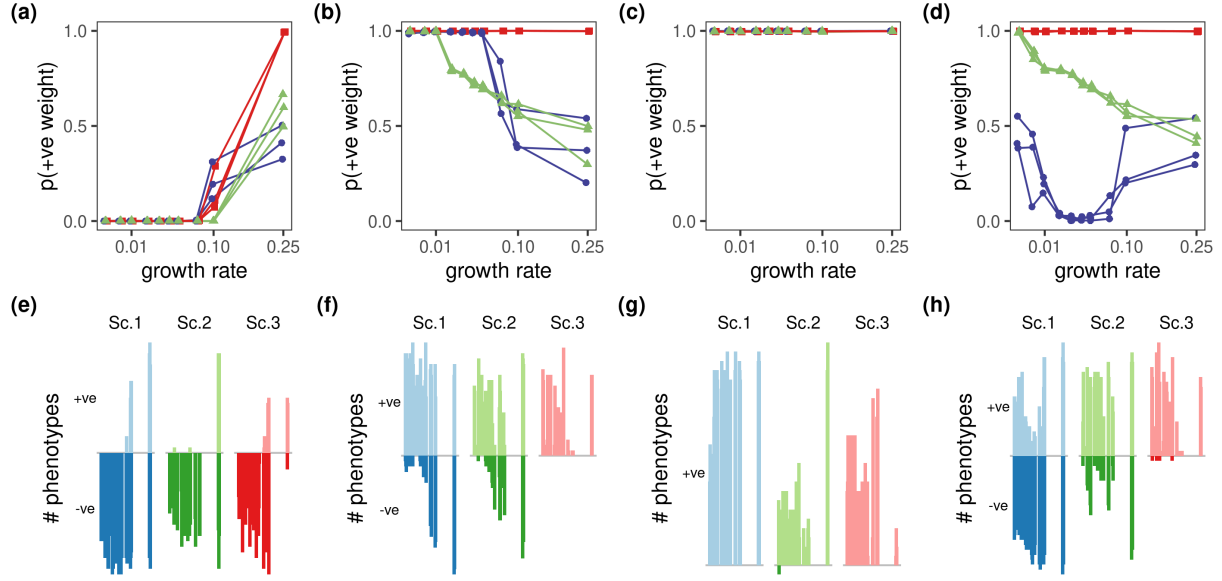


Figure 1: Proportion of individuals in populations evolved across different regrowth rates selecting for environmental cues in deciding movement. Panels (a – d) show the proportion of individuals with positive weights for each cue: (a) non-handling individuals, (b) handling individuals, (c) prey items, and (d) individuals overall. Colours and shapes represent scenarios (blue circles: *producers-only*; green triangles: *fixed-strategy*; red squares: *flexible-strategy*). While lines connect similarly numbered replicates across r_{base} , these are entirely independent simulations. Panels (e – h) show the number of distinct values for each weight in the population in panels (a – d) separated by the sign (positive or negative): (e) non-handling individuals, (f) handling individuals, (g) prey items, and (h) individuals overall. Bar colours represent scenarios (blue: *producers-only*; green: *fixed-strategy*; red: *flexible-strategy*), while the hue represents the sign (light: positive, dark: negative). Individuals avoid non-handlers for $r_{base} \leq 0.1$, after which they evolve neutrally in scenarios 1 and 2, and strongly positive values in scenario 3 (a, e). Similarly, most individuals in scenarios 1 and 2 move towards handlers, but the proportion and diversity of negative weights increases at $r_{base} \geq 0.1$ (b, f). Individuals in scenario 3 consistently move towards handlers, and individuals overall (b, f, d, h). Overall, in scenario 1 individual preference for moving towards other individuals has an inverse-humped relationship with r_{base} , while in scenario 2 it shows a steady linear decline.

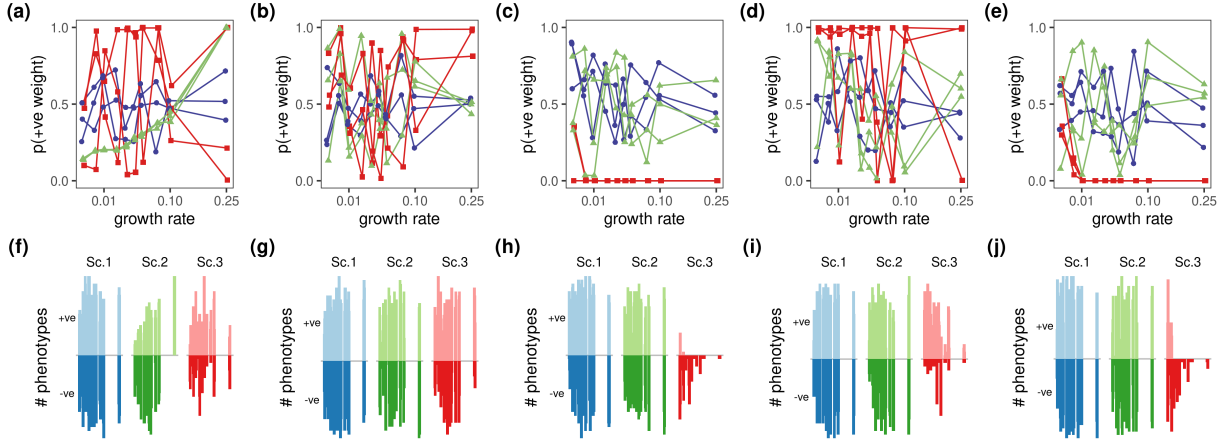


Figure 2: The proportion of individuals choosing a foraging strategy based on environmental cues is not linked to the regrowth rate. Panels (a – e) show the proportion of individuals with positive weights for each cue: (a) bias, (b) non-handling individuals, (c) handling individuals, (d) prey items, and (e) all cues combined. Colours and shapes represent scenarios (blue circles: *producers-only*; green triangles: *fixed-strategy*; red squares: *flexible-strategy*). Lines connect similarly numbered replicates across r_{base} , but these are entirely independent simulations. Panels (f – j) show the number of distinct values for each weight in the population in panels (a – e) separated by the sign (positive or negative): (f) bias, (g) non-handling individuals, (h) handling individuals, (i) prey items, and (j) all cues combined. Bar colours represent scenarios (blue: *producers-only*; green: *fixed-strategy*; red: *flexible-strategy*), while the hue represents the sign (light: positive, dark: negative). Individuals' weights in scenario 1 evolve neutrally since they are only allowed a producer strategy. However, scenario 2 also results in neutral evolution of all weights except f_b , with a larger proportion of individuals biased towards producing at high r_{base} . Almost all individuals in scenario 3 choose to steal except at very low r_{base} , with f_h the strongest contributor to the decision.